Soft Matter

Accepted Manuscript

This is an *Accepted Manuscript*, which has been through the Royal Society of Chemistry peer review process and has been accepted for publication.

Accepted Manuscripts are published online shortly after acceptance, before technical editing, formatting and proof reading. Using this free service, authors can make their results available to the community, in citable form, before we publish the edited article. We will replace this *Accepted Manuscript* with the edited and formatted *Advance Article* as soon as it is available.

You can find more information about *Accepted Manuscripts* in the Information for Authors.

Please note that technical editing may introduce minor changes to the text and/or graphics, which may alter content. The journal's standard Terms & Conditions and the Ethical guidelines still apply. In no event shall the Royal Society of Chemistry be held responsible for any errors or omissions in this *Accepted Manuscript* or any consequences arising from the use of any information it contains.

ROYAL SOCIETY OF CHEMISTRY

www.rsc.org/softmatter

Thermo-responsive properties driven by hydrogen bonding in aqueous cationic gemini surfactant systems

Xi-Lian Wei,* Chuan-Hong Han, Pei-Pei Geng, Xiao-Xiao Chen, Yan Guo, Jie Liu, De-Zhi Sun, Jun-Hong Zhang, Meng-Jiao Yu

Shandong Provincial Key Laboratory of Chemical Energy Storage and Novel Cell Technology, College of Chemistry and Chemical Engineering, Liaocheng University, Liaocheng, Shandong 252059, P. R. China

Abstract A series of unexpected thermo-response phenomena were discovered in an aqueous solution of the cationic gemini surfactant, 2-hydroxypropyl-1,3-bis(alkyldimethylammonium chloride) (n-3(OH)-n(2Cl), n = 14, 16), in the presence of an inorganic salt. The viscosity change trend for the 14-3(OH)-14(2Cl) system was investigated in the 20-40°C temperature range. As the temperature increased, the viscosity of the solution first decreased to a minimum point corresponding to 27°C, and then increased until a maximum was reached, after which the viscosity decreased again. In the 16-3(OH)-16(2Cl) system, the gelling temperature (T_{gel}) and viscosity variation trend upon heating were similar to those in the 14-3(OH)-14(2Cl) system above 27°C. The reversible conversion of elastic hydrogel to wormlike micelles in the aqueous solution of 16-3(OH)-16(2Cl) system in the presence of inorganic salt was observed at relatively low temperatures. Various techniques were used to study and verify the phase-transition processes in these systems, including rheological measurements, cryogenic transmission electron microscopy (cryo-TEM), electric conductivity, and differential scanning calorimetry. These phenomena were explained by the formation and destruction of intermolecular hydrogen bonds, and the transition mechanisms of the aggregates were analyzed on this basis.

* Shandong Provincial Key Laboratory of Chemical Energy Storage and Novel Cell Technology, Liaocheng University, Liaocheng, Shandong 252059, P. R. China
E-mail: weixilian@126.com; Fax: +86-635-8239196; Tel: +86-635-8230613

Soft Matter Accepted Manuscript

Introduction

In recent years, smart wormlike micelles (SWLMs) have attracted considerable attention due to their theoretical significance and potential industrial applications in many areas.[1] SWLMs are formed by introducing functional groups that respond to environmental stimuli into the surfactant molecular structure; alternatively, some components capable of participating in micellar assembly and responding to environmental stimuli can be introduced into the system. In either case, a micellar system that responds to external environmental stimuli is produced. The environmental stimuli include temperature,[2,3] illumination,[4,5] pH,[6,7] gases,[8,9] electric field,[10] force field,[11] additives,[12,13] and other comprehensive factors.[14,15] Temperature is one of the most easily controlled factors; in fact, regulating temperature is not only simple but also beneficial to environment since no chemical agent is added to the system. As an effective and convenient method, temperature modulation/control has been used to regulate the formation and properties of SWLMs.[1]

Temperature generally affects the viscosity of wormlike micellar systems in the following two ways. First, the micellar contour length decays exponentially upon increasing the temperature, leading to an exponential decrease in zero-shear viscosity η_0, which is in accordance with Arrhenius' law. Most wormlike micellar systems behave in this way. Second, thermo-thickening and thermo-thinning behaviors are observed at low and high temperatures, respectively; namely, the curve of η_0 as a function of temperature usually has a maxima. Such systems, whose viscosity increases in response to heat stimuli, are referred to as temperature-responsive or thermo-responsive systems. Different types of surfactants, such as cationic,[2, 16–22] nonionic,[23–26] anionic,[27-29] and amphoteric surfactants,[3, 30,31] can be used to produce thermo-responsive wormlike micelles, although thermo-responsive systems formed using cationic gemini surfactants have been documented less often. [32]

Gemini quaternary ammonium salt (GQAS), a kind of cationic surfactant, is a chemical compound containing two amphiphiles that are connected (bonded) at or near their polar headgroups by a spacer group.[33] Because this type of gemini surfactants have better properties than traditional monoalkyl cationic surfactants, which are formed with a hydrophilic group, they are increasingly favored by researchers.[34,35] Unlike single-chain

Soft Matter Accepted Manuscript

surfactants, the rheology of cationic gemini surfactant aggregates is not only related to the length of the hydrophobic chain, hydrophilic headgroup, and the type of counter-ion but is also dependent on the structure of the spacer group. Thus, in-depth studies on the rheological properties of different cationic gemini surfactants in aqueous solutions and their mixed systems with additives are of great importance for practical applications.

By studying the phase behavior and general rheological properties of a cationic gemini surfactant 2-hydroxypropyl-1,3-bis (alkyldimethylammonium chloride) [$C_nH_{2n+1}-N^+(CH_3)_2-CH_2CH(OH)CH_2-N^+(CH_3)_2-C_nH_{2n+1}]2Cl^-$ (hereafter abbreviated as n-3(OH)-n(2Cl), where n = 12, 14, and 16; the molecular structure is shown in Scheme 1),[36-38] we further investigated the impact of temperature changes and the addition of an inorganic salt on the viscoelasticity.

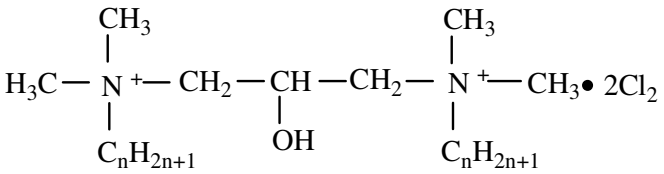

Scheme 1 Molecular structures of cationic gemini surfactants n-3(OH)-n(2Cl), n = 12, 14, and 16

We were surprised to find that n-3(OH)-n(2Cl) systems were not only thermo-responsive, but also exhibited a series of other special properties. Indeed, upon increasing the temperature, the viscosity of some pure solutions increases within a certain temperature range. Solutions of some of the systems form hydrogels at low temperatures and undergo abrupt transitions to micelle solutions at specific temperatures. At very low concentrations, the 16-3(OH)-16(2Cl) solution forms gel systems upon addition of inorganic salt and similarly transitioned into wormlike micelles at specific temperatures. This series of interesting thermo-response phenomena aroused our interest in these systems.

In this work, the rheological properties of both pure and mixed systems of n-3(OH)-n(2Cl) in the presence of an inorganic salt have been systematically studied by varying the temperature and additive concentration. Additionally, the underlying reasons for their phase and structural transitions have been analyzed. Our aim is to understand the relationship

Soft Matter Accepted Manuscript

between the rheological behaviors and molecular structures, and to provide useful experimental data for the applications of these systems in different fields.

Experimental

Materials

2-hydroxypropyl-1,3-bis (alkyldimethylammonium chloride) (n–3(OH)–n(2Cl), n = 14 and 16, as shown in Scheme 1) were synthesized and purified in our laboratory according to the methods reported in the literature;[36,37] the other compounds were purchased from the Shanghai Aladdin Chemical Co. and were of A.R. grade. The water used in solution preparation was redistilled from alkaline potassium permanganate, whose electrical conductivity was 1.10 μs·cm^{-1} at 20°C.

Apparatus and experimental procedure

Rheological measurements. Samples for rheological measurements were prepared in pure water by weighing the required amount of sample and were stirred well to ensure homogenization they were left in a water bath at the desired temperatures for at least 48 h to ensure equilibration. Rheological measurements of all the samples were performed using a stress- controlled rheometer (AR2000ex, TA instruments, USA). Cone (20 mm) and plate (20 mm) geometries were used in each case. The temperature was controlled at $T \pm 0.05$°C using a Peltier plate for all the temperatures considered in this work. A solvent trap was used to minimize water evaporation. Dynamic frequency spectra were obtained in the linear viscoelastic regime of the samples, which was determined from dynamic stress sweep measurements. For steady-shear measurement, sufficient time was allowed before data collection at each shear rate to ensure that the viscosity reached its steady-state value. Each measurement was repeated thrice to ensure good reproducibility.

Cryogenic Transmission Electron Microscopy (Cryo-TEM). The wormlike micelles were observed by cryogenic transmission electron microscopy (cryo-TEM). The samples for cryo-TEM were prepared in a controlled-environment vitrification system (Cryoplunge 3, Gatan, USA) at room temperature. For producing the thin film, 1 μL solution was placed on a copper grid coated with carbon film, and the redundant liquid was blotted off with filter paper. Then, the thin film was produced. Subsequently, the thin film was quickly plunged into liquid

Soft Matter Accepted Manuscript

ethane cooled by liquid nitrogen. The vitrified sample was placed in a cryogenic specimen holder and examined using a JEOL JEM 1400 TEM at 120 KV.

The electric conductivity of the surfactant solution was measured over the 10–50°C temperature range using a Model DDS-308A conductivity meter. The DSC measurements were carried out at 1°C min-1 using a Pyris Diamond DSC (Perkin Elmer, US) instrument.

Results and discussion

Thermo-responsive properties

Aqueous systems of n–3(OH)–n(2Cl) with different hydrophobic chain lengths exhibit different responses when subjected to temperature changes. For the system with n = 12, the viscosity of the solution gradually decreases with temperature enhancement,[36] which was in agreement with Arrhenius' law. For the other two surfactant systems with n = 14 and 16, the respective hydrophobic chains differ by two carbon atoms; consequently, they exhibit substantial variations in their appearance and viscoelastic behavior in solution. The solution system of the surfactant with n = 14 is always transparent, regardless of concentration. Additionally, it appears as an isotropic liquid when observed under a polarizing microscope and exhibits a birefringent phenomenon when the sample vial is tilted. The viscosity curve of the solution presents interesting changes as the temperature increases. In contrast, the system of the surfactant with n = 16 appears as an opalescent gel at low temperatures. Hence, the viscosity changes for this system were studied at higher temperatures, and the gel formed by this system will be discussed separately.

The zero-shear viscosities (η_0) for different concentrations of n–3(OH)–n(2Cl), where n = 14 and 16, under various temperatures are shown in Fig. 1. For the solution of the surfactant with n = 16, the viscosity increases continuously upon increasing temperature until a maximum is reached, after which the viscosity decreases with temperature enhancement. This behavior is similar to that of the solutions of other surfactants both with and without additives.[16, 39-42]

Soft Matter Accepted Manuscript

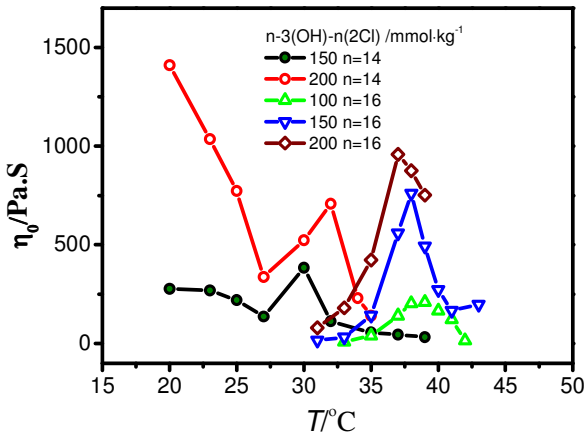

Fig. 1 Zero-shear viscosity (η_0) of the n-3(OH)–n(2Cl) solution as a function of temperature (T) at different concentrations. ■ and ● are 100 and 200 mmol·kg^{-1} 14-3(OH)–14(2Cl); ▲,▼, and ◆ are 100, 150, and 200 mmol·kg^{-1} 16-3(OH)–16(2Cl).

Surprisingly, the viscosity of the surfactant solution with n = 14 decreases upon heating if the temperature is lower than 27°C. The η_0 is the lowest at this temperature, but subsequent changes are similar to those observed for n = 16. Regarding the external appearance, these solutions are gelatinous at low temperatures and then change into a fluid state at 27°C. On increasing the temperature further, the viscosity also increases, and the solutions concomitantly become sticky (Fig. 2c). These changes are similar to those reported by Raghavan et al., who studied the states of a cationic surfactant with long unsaturated tails (also known as EHAC) and sodium salicylate (NaSal) under low and high temperatures.[20]

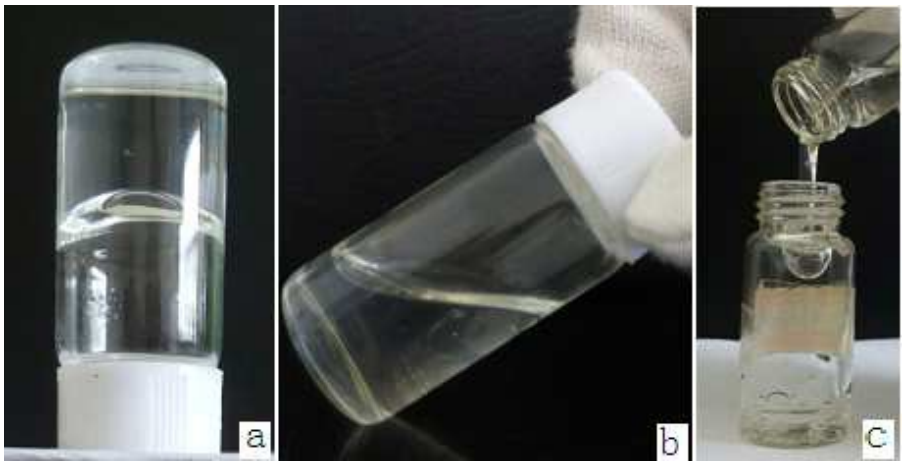

Soft Matter Accepted Manuscript

Fig. 2 Appearance of an aqueous solution of 14-3(OH)-14(2Cl) with 200 mmol·kg^{-1} concentration at different temperatures, viz. (a) 23°C, (b) 27°C, and (c) 32°C.

Raghavan et al. reported that the unsaturated long chain of EHAC itself exhibited low critical micellar concentration (cmc) and high water solubility. After mixing with NaSal, the overlap concentration C^* was greatly reduced. The hydrophobicity of the long chain caused the system to form cylindrical micelles with a high end-cap energy, (the energy cost for micellar scission), Ec, which facilitated the micellar growth. The gel-like appearance at low temperature could be attributed to the extra-long relaxation times, τ_R, and ω_c is too low to measure within the frequency range of the dynamic rheology profile. In contrast, for the 14–3(OH)–14(2Cl) system below 27°C, all dynamic curves of the gelatinous state had intersection points within the frequency range, and the relaxation time, τ_R, could be determined.

Fig. 3 is the frequency sweep curve for the solution of 14–3(OH)–14(2Cl) at 200 mmol·kg^{-1} concentration. The elastic and viscous moduli (G' and G'', respectively) increase with shear frequency (ω), but deviate from the Maxwellian model at high frequencies. This observation was in agreement with previous studies, showing that wormlike micelles [30–31] typically exhibit a singular relaxation time. The solid lines are produced by fitting with the Maxwellian model. The change trends for the elastic and viscous moduli shown by the various curves at 27°C and above are consistent with the literature.[20,21,39-42]

Soft Matter Accepted Manuscript

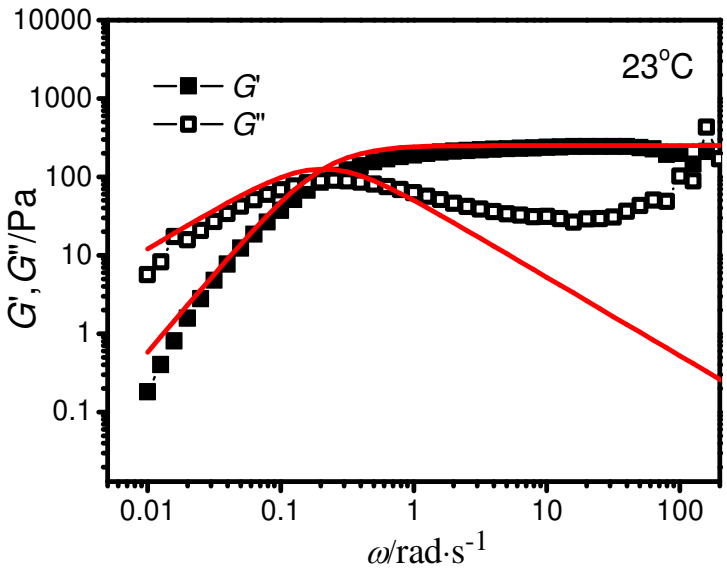

Fig. 3 Variations in the elastic G'(filled symbols) and viscous moduli G'' (open symbols) versus dynamic frequency (ω) for the 200 mmol·kg^{-1}14–3(OH)–14(2Cl) solution. The solid lines represent the best fit to the Maxwellian model at 23°C.

The same viscosity variation trends on increasing temperature have been reported previously for a cationic gemini surfactant solution with a similar structure.[32] However, the study provided only three experimental points. The increase in viscosity with temperature can be explained as follows. The different spherical aggregates (vesicles and micelles) that coexist in the system at low temperatures change their structures into wormlike micelles on increasing the temperature. Our results should be related to the hydroxyl group embedded in the spacer group of the gemini surfactant molecules. Hence, cryo-TEM observations were performed.

A photograph of the microstructure at 25°C clearly shows that the 14–3(OH)–14(2Cl) system contained long cylindrical micelles. This system exhibited a fingerprint-like oriented alignment (Fig. 4a), and the diameter of the micelles was less than 10 nm. These findings are very similar to the microstructure of the hexadecyltrimethylammonium 2, 6-dichlorobenzoate system.[43] However, the reason for the formation of this structure has not been reported previously.

Soft Matter Accepted Manuscript

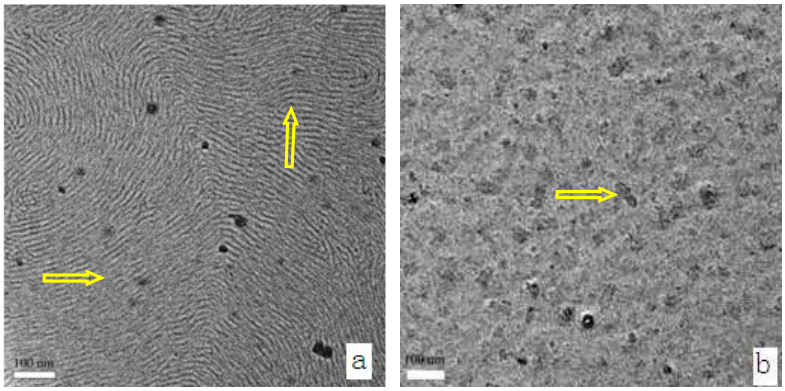

Fig. 4 Cryo-TEM images of solutions at 25ºC; (a) 200 mmol·kg^{-1} 14-3(OH)–14(2Cl) and (b) 150 mmol·kg^{-1}16-3(OH)–16(2Cl). Arrows indicate some micelle end points.

By combining this observation with the dynamic and steady-state curves, a possible explanation was posited for the unusual changes in solution viscosity, which first decreases, then increases with increasing temperature until the maximum is reached, and then decreased again. Previous studies[36,37] have shown that in the crystalline state, the chloride ions and hydroxyl groups of the bridging groups in C_n–3(OH)–$C_n(Cl_2)$ molecules and crystallization water molecules form upright hydrogen bonds, resulting in a herringbone-like structural arrangement.[37] Such hydrogen bond links persisted at low temperatures, even after the surfactant in the aqueous solution had formed cylindrical micelles because of the hydrophobic effect. The counterions were not tightly adsorbed into the micellar interfaces. Because the steric hindrance of these links did not facilitate the entanglement of the wormlike micelles, the system showed regularly oriented alignment with an appearance similar to that of fingerprints, thus endowing a fixed surface to the cylindrical micelles (Fig. 2a); consequently, the macroscopic appearance became more viscous (20–27°C).

When the temperature was increased, the hydrogen bonds were first disrupted, leading to the release of counterions. Then, the cylindrical micelles entered a dissociated state (Fig. 2b), and the viscosity of the solution decreased. After the viscosity was minimized, continuous temperature increase led to disordering of the micelles, and the end-cap energy of the rod-like micelles increased. The wormlike micelles, which originally exhibited an oriented alignment, became intertwined and formed a network structure. The macroscopic appearance of the solution also became more viscous, and the viscosity was then maximized at specific and

Soft Matter Accepted Manuscript

narrow temperature ranges. When the temperature was increased further, the dynamic characteristics of the wormlike micelles caused the network structure to break down, leading to the formation of rod-like micelles with smaller dimensions or spherical ones. As the relaxation time of the system decreased, the viscosity of the solution also decreased. A possible mechanism for the changes in micellar dimensions from the lower temperatures to the higher temperature, at which the viscosity was maximized, is shown in Fig. 5.

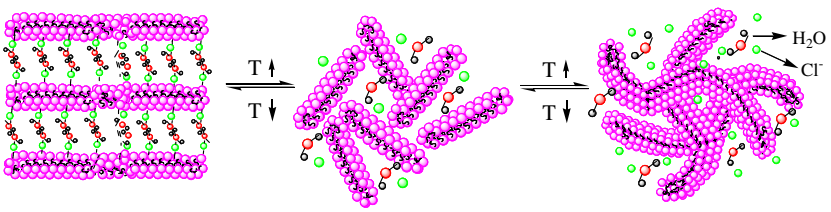

Fig. 5 Mechanism of micellar formation in the 14–3(OH)–14(2Cl) solution at low and high temperatures

Thermo-responsive sol–gel transition

Regarding the microscopic structure of the solution of 16–3(OH)–16(2Cl) with 150 mmol·kg^{-1} concentration, only rod-like micelles with lengths of approximately 40–50 nm and diameters that were much bigger than those of 14–3(OH)–14(2Cl) were observed (Fig. 4b). These differences can probably be attributed to the fact that the solution of 16–3(OH)–16(2Cl) was in a translucent gelatinous state at room temperature. It did not exhibit any textural characteristics of lyotropic liquid crystals when viewed under crossed polars, and was identified as a surfactant hydrogel. Thus, we were unable to observe any clear micellar forms at room temperature. Hence temperatures of 30°C and above were selected to investigate the impact of temperature on the viscosity of 16–3(OH)–16(2Cl). However, it should be noted that because of the limitations of the experimental conditions, we did not perform electron microscopy observation for the sample at high temperatures.

For the 16–3(OH)–16(2Cl) gelatinous system subjected to increasing temperature, solutions of different concentrations suddenly changed from translucent gelatinous solid state to a transparent free-flowing solution at specific temperatures. As the temperature was raised

Soft Matter Accepted Manuscript

further, the systems became transparent viscoelastic solutions. The appearance of the solution of 16–3(OH)–16(2Cl) with 150 mmol·kg^{-1} concentration at 30, 31, and 35°C is shown in Figs. 6a–c, respectively. Even when inverted, the samples in Fig. 6a (gel) and 6c did not flow. Thus, we conducted further studies on the gelatinous solution of the 16–3(OH)–16(2Cl) system. We were surprised to find that the different solutions exhibited reversible thermal transitions from opalescent gels to transparent solutions at approximately equivalent specific temperatures.

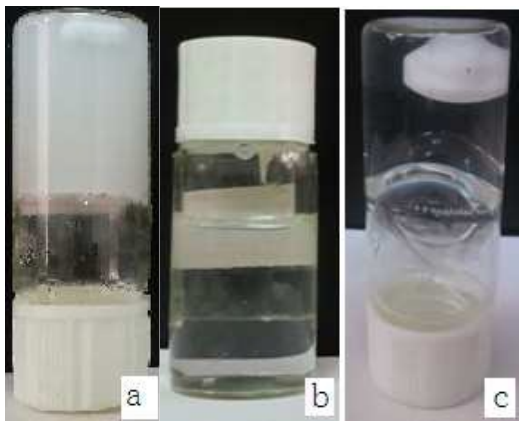

Fig. 6 Macroscopic appearance of the solution of 16–3 (OH)–16(2Cl) with 150 mmol·kg^{-1} concentration at different temperatures, viz. (a) 30°C, (b) 31°C, and (c) 35°C

Furthermore, we performed electric conductivity tests to verify the transition. The electric conductivity curves of different concentrations of 16–3(OH)–16(2Cl) as functions of temperature are shown in Fig. 7. The electric conductivity of solutions at three concentrations (100, 150, and 200 mmol·kg^{-1}) all exhibited inflection points indicating dramatic increases at 29, 30, and 31°C, respectively. This observation indicated that a sudden increase in the concentration of free ions occurred in the solution corresponding to these points. The inflection point also corresponds to the temperatures at which the solutions change from opalescent gels to transparent solutions. After the sudden increase, the change in the electric conductivity became relatively gradual. Based on the curves, the inflection point should not be the Krafft point of the surfactant. Our determined value was – (3.0±0. 5) °C, being in accordance with that reported by literature [44]. Hence, the sudden change in the electric conductivity value is likely due to the structural transition of the morphology of the

Soft Matter Accepted Manuscript

aggregates in the solutions. Specifically, at this temperature, the hydrogel transitioned to wormlike micelles; this temperature is known as the gelation temperature (T_{gel}).[18]

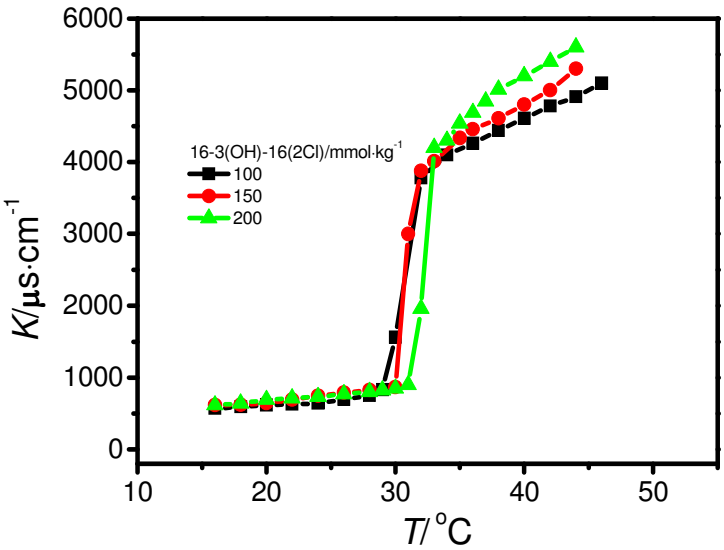

Fig. 7 Electric conductivity of 16-3(OH)–16(2Cl) solutions (κ) as a function of temperature (T) at different concentrations shown in the diagram.

The mechanism of gel formation was probably based on the hydrogen bonds formed between the counterion (Cl^-), hydroxyl groups of the bridging groups, and water molecules. Hydrogen bonds, which caused the interlinking of rod-like micelles, are also one of the most common types of noncovalent bonds that occur when a low-molecular weight gelling agent forms a gel.[45] These bonds caused the micelles to form relatively regular crystallized interfaces and immobilized the wormlike micelles. Hence, the counterions contributed to the electric conductivity in a small way by binding to the surfaces of the micelles. Furthermore, before the inflection point (Fig. 7), a small amount of counterions was desorbed into the solution as the temperature increased, which slightly increased the electric conductivity.

When the temperature rose to the gel temperature, thermal motion caused the hydrogen bonds between the counterion, hydroxyl groups, and water molecules to break. The immobility of the molecules on the surfaces of the micelles was similarly disrupted. Thus, the rod-like micelles entered a free state. The increased release of chloride ions from the surfaces of the micelles into the solution results in a sudden increase in the electric conductivity. After

Soft Matter Accepted Manuscript

reaching a specific value, the remaining counterions are gradually released as the temperature continues to rise. Correspondingly, the rate of increase in the electric conductivity also slows. At this point, the release of counterions prompts the rod-like micelles to increase their lengths in a unidimensional direction, generating longer wormlike micelles. The viscoelastic behavior of the solution with respect to temperature shows a corresponding change trend, as depicted in Fig. 1. The rheological profile of the solution confirmed that the nature of this type of solution changes on increasing the temperature.

The dynamic curves of the 16–3(OH)–16(2Cl) solution with 100 mmol·kg^{-1} concentration at different temperatures are shown in Fig. 8. As the temperature rose (Fig. 8a), the elastic and viscous modulus of the solution and its composite viscosity | η* | all decreased to a minimum

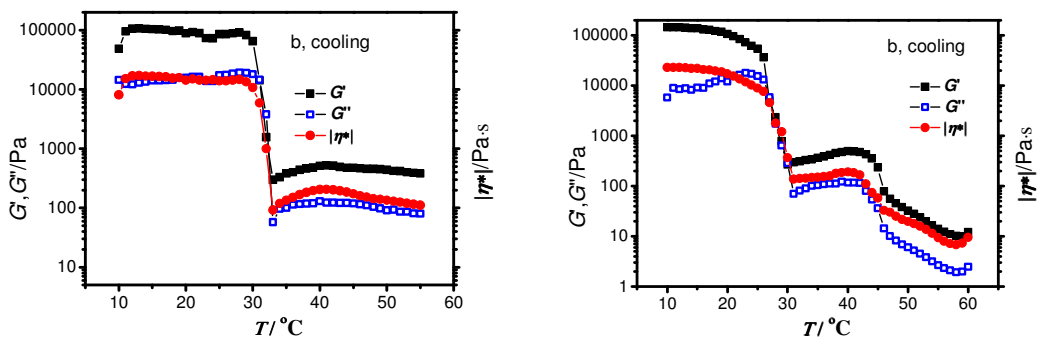

Fig. 8 Dynamic rheological curves of the100 mmol·kg^{-1}16-3(OH)–16(2Cl) solution as a function of temperature, (a) heating process; (b) cooling process

value at approximately 30°C before subsequently increasing slightly. These changes were consistent with the results of the electric conductivity measurements and the situation was shown in Fig. 1. However, unlike the situation shown in Fig. 1, change in viscosity value was not very obvious within the temperature range of 30~40°C upon heating, which could be related to the following. The viscoelasticity of the system may not have reached equilibrium during the scanning process, as the temperature increased because of the settings used for various parameters of the solution and delays in system's response. During the experiment, the rate of temperature increase was set to 1°C/min. Rheological experiments are usually performed at constant temperature to ensure that equilibrium is reached. Hence, even when the sample temperature reached a certain level during the temperature sweep experiment, it

Soft Matter Accepted Manuscript

might not completely reflect the trend of changes in real equilibrium states in the narrow temperature ranges. Nevertheless, the sol–gel transition and the changing trends of both moduli（*G*'and *G*"）and ｜η*｜ as functions of the temperature after the transition could be clearly observed. Simultaneously, in order to verify the reversible performance of phase transformation, an experiment of cooling process was conducted (Fig. 8b). The reversible changes corresponding to the heating process were observed on cooling curves and the transitions from small micelles to wormlike micelles were obvious as cooling.

The dynamic rheological profiles of 16–3(OH)–16(2Cl) solution with 150 mmol·kg^{-1} concentration at different temperatures in the sol and gel states are shown in Fig. 9a–b. At 30°C and a stress range of 0.04–60 Pa (Fig. 9a), the elastic modulus (*G′*) of the solution was always greater than the viscous modulus (*G″*). The system was primarily elastic, demonstrating the stability of the gel. The opposite behavior occurred at 31°C, and the viscosity was slightly greater than the elasticity, indicating that the system had changed from an elastic gel to viscous micelles. This is a characteristic stress curve of the rod-like micelles. When the temperature rose to 35°C, the system again appeared to be primarily elastic, indicating that the wormlike micelles had interlinked.

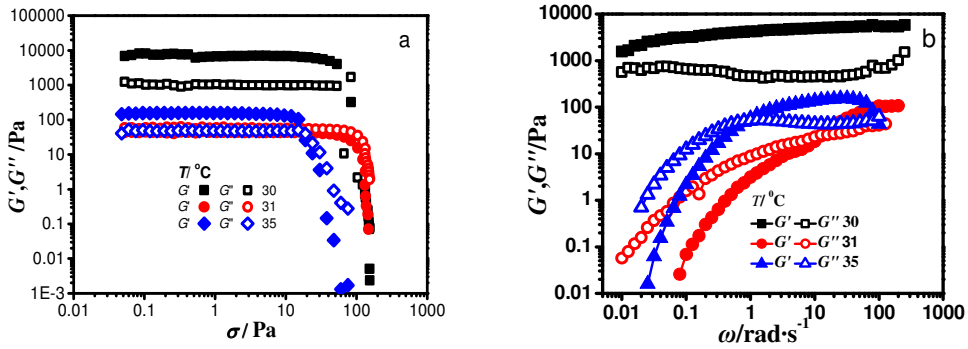

Fig. 9 (a) Stress and (b) frequency sweep curves of 16–3 (OH)–16(2Cl) solution with 150 mmol·kg^{-1} concentration at 30°C, 31°C, and 35°C

In Fig. 9b, it can be seen that the elastic modulus (*G*') of the gel state was always greater than the viscous modulus (*G*") at 30°C within the measured frequency range. Similar behavior was observed in the frequency curve of the hydrogel formed by adding salt to a

Soft Matter Accepted Manuscript

surfactant,[46–48] indicating that the system had an extremely long relaxation time t_R or extremely high viscosity. The steady-state viscosity curve did not include a Newtonian plateau zone, while the storage modulus was greater than that at 31°C by as much as an order of magnitude. The frequency sweep curve at 31°C was consistent with the characteristics of rod-like micelles,[49] with the system had a shorter relaxation time and lower viscosity. However, the frequency curve exhibited characteristics of wormlike micelles at 35°C. Overall, the system was consistent with the Maxwell model at low and medium frequencies but deviated from the model at high frequencies,[1–14] similar to the situation depicted in Fig. 3. The deviation at high frequencies was caused by the Rouse motion of the system, which became significant at high frequency.[50] More interestingly, these systems were found to be reversible. By repeatedly raising and lowering the temperature, the appearance of the system could be switched between being opalescent and transparent. The rheological curve of the system also exhibited reversibility.

A thermal effect should evidence the transition of the gel to micelles. Thus, we conducted differential scanning calorimetry (DSC) measurements to confirm the transition. The DSC curve of a 5-mg sample of the 16–3(OH)–16(2Cl) solution (100 mmol·kg^{-1}) is shown in Fig. 10. On the heating curve, two endothermic peaks appeared at 30 and 37°C, respectively. The first endothermic peak shows the change of gel to micelle, which is consistent with the sudden changes in temperature observed in the electrical conductivity measurement (Fig. 7) and the temperature sweep curve (Fig. 8). This temperature corresponded to the transition temperature from the gel to micelles. The second peak is at the temperature corresponding to the peak viscosity, which belongs to the endothermic process caused by the entangled micelle fracture. These changes were consistent with the results of the dynamic rheological measurements at different temperatures. However, the big exothermic peak was observed from 34°C to 25 °C and the small one from 37°C to 35 °C in the cooling curve. It could be seen that the bigger peak corresponding to the regaining of the gel became flat and wide while the smaller one corresponding to the assembly of short-rod micelles into entangled micelles became even smaller. This phenomenon means that the change of the aggregates from short-rod micelles to entangled micelles with the temperature descending is not as obvious as the reverse process with the temperature ascending. This is likely due to existence

Soft Matter Accepted Manuscript

of subcooled short-rod micelles in the system，leading to the time delay for the regeneration of the entangled micelles. Perhaps a very slow cooling rate can make the curve of cooling symmetrical with the one of heating. However, because of the limitation of the function of the DSC calorimeter, such a measurement cannot be performed. But the phase transition from dissociated micelles to sol–gel was still reversible under cooling. The slight shift of the exothermic peak was caused by the time delay needed for the phase transition.

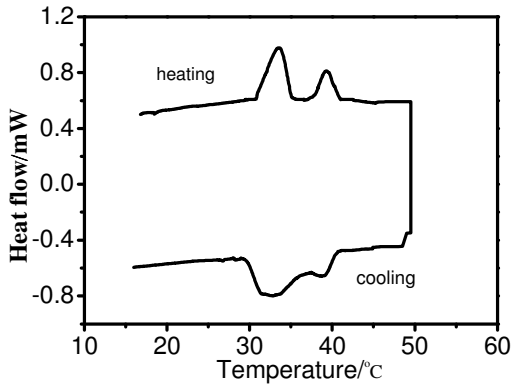

Fig. 10 DSC heating and cooling curves of aqueous solutions of 16–3(OH)–16(2Cl) at 100 mmol·kg^{-1}.

Formation of 16–3(OH)–16(2Cl)/NaCl mixed hydrogel

When excessive amounts of inorganic salt (NaCl) and organic salt (for example, sodium salicylate, sodium p-hydroxybenzoate) were added to a dilute solution (such as 10 mmol·kg^{-1}) of 16–3(OH)–16(2Cl) at room temperature, all the mixed systems containing organic salt dissolved at high temperatures and generated pale-blue vesicular solutions. Precipitation occurred when the system was cooled to room temperature, and the precipitation was reversible (this behavior will be studied in a separate paper). This phenomenon was caused by the strong electrostatic effect between the positive and negative ions.

In contrast, those mixtures containing NaCl were able to form a reversible gel system. Different concentrations of NaCl (20, 40, 60, and 80 mmol·kg^{-1}) were added to the solution of 16–3(OH)–16(2Cl) with 10 mmol·kg^{-1} concentration. We first observed that all four systems had an opalescent jelly-like appearance at room temperature (similar to that shown in Fig. 6a). An ultra-thermostat was used to gradually raise and lower the systems' temperatures. The temperature (T_{gel}) at which the gel suddenly became a transparent solution was repeatedly

Soft Matter Accepted Manuscript

detected. Additionally, we also measured the rheological profiles at two temperatures when the systems were in the gel and solution states. The shapes of the curves were similar to that of the 100 mmol·kg^{-1} solution of 16–3(OH)–16(2Cl). The obtained rheological parameters are shown in Table 1.

Table 1. T_{gel} and Some rheological parameters of 16–3(OH)–16(2Cl)/NaCl mixed solution

Number	C_{NaCl}	T_{gel}	η_0 /Pa·s		G_0/Pa		t_R/s	
	mmol·kg^{-1}	^{o}C	hydrogel	solution	hydrogel	solution	hydrogel	solution
1	20	36	52.89	3.923	22880	1.336	∞	1.585
2	40	37	13.42	1.917	15090	1.491	∞	2.893
3	60	38	8.392	1.264	525	1.407	∞	3.059
4	80	39	9.349	1.441	493	1.265	∞	4.435

As can be seen from Table 1, T_{gel} and t_R (relaxation time of the micellar solution) gradually increased with increasing salt concentration. In contrast, the zero-shear viscosity η_0 and plateau modulus G_0 of the gel decreased with the addition of salt. Furthermore, the values of η_0 and G_0 for the gel system were much higher than those of the micellar solution. Taken together, these results show that addition of NaCl to a dilute solution of 16–3(OH)–16(2Cl) weakens the adsorption force between the counterions and the surfactant headgroups. Simultaneously, this additive can reduce the repulsion between the polar headgroups and thus facilitated the formation of rod-like micelles within the system. These micelles crystallized at low temperatures, resulting in an oriented alignment and the formation of a hydrogel. The release of counterions as the temperature increased then led to the generation of viscoelastic wormlike micelles. These observations prompted us to study the use of low-concentration surfactants and inexpensive inorganic salt to create hydrogels quickly and easily.

Conclusions

In summary, a series of thermo-responsive phenomena were discovered in a cationic gemini surfactant solution. Within a specific temperature range, the zero-shear viscosities of different solutions of n-3(OH)-n(2Cl), where n = 14 and 16, increased with increasing temperature and then decreased after reaching a maximum value. These changes were related to the hydrogen bonds that were formed between the hydroxyl group, counterions, and water molecules in the

Soft Matter Accepted Manuscript

solution. As the temperature increased, the zero-shear viscosity of 14–3(OH)–14(2Cl) solution exhibited undulating behavior, which was related to the immobilization of the rod-like micelles because of the hydrogen bonding effect at low temperatures and the disruption of those hydrogen bonds at higher temperatures. For the 16–3(OH)–16(2Cl) solution, which generated short rod-like micelles at low temperatures, a transition process from gel to micellar solution occurred at approximately T_{gel}. The formation of the gel was similarly related to the hydrogen bonds in the systems. The gel formed by adding inorganic salt to a dilute 16–3(OH)–16(2Cl) solution and the conditions of the sol–gel transition were similar to those of surfactant systems without any additive. Both the rheological profiles and electric conductive measurements of the solution confirmed the changes described above. We hope that this study will contribute to a better understanding of the relationship between the introduction of functional groups in surfactant molecules and the macroscopic properties of their solutions. Such an understanding would facilitate the appropriate selection of surfactants for practical applications and the realization of control over transitions between ordered structures through a simple temperature-regulation method.

Acknowledgments

This work was supported by the National Natural Science Foundation of China and Shandong Province (Grant No. 21473084, 21373106, 21073081, ZR2012BQ013); Key Topics for Scientific Research (314011402), Experimental Technology Projects (LDSY2014008) and Teaching Research of Liaocheng University.

References

1 Z. L. Chu, C. A. Dreiss and Y. J. Feng, *Chem. Soc. Rev.*, 2013, **42**, 7174–7203.

2 T. S. Davies, A. M. Ketner and S. R. Raghavan, *J. Am. Chem. Soc*., 2006, **128**, 6669 – 6675.

3 Z. L. Chu and Y. J. Feng, *Chem. Commun*., 2011, **47**, 7191–7193.

4 H. Y. Lee, K. K. Diehn, K. S. Sun, T. H. Chen and S. R. Raghavan, *J. Am. Chem. Soc.*, 2011, **133**, 8461–8463.

5 Y. Y. Lin, X. H. Cheng, Y. Qiao, C. L. Yu, Z. B. Li, Y. Yana and J. B. Huang. *Soft Matter*, 2010, **6,** 902–908.

Soft Matter Accepted Manuscript

6 L. Zhao, K. Wang, L. M. Xu, Y. Liu, S. Zhang, Z. B. Li, Y. Yan and1, J. B. Huang, *Soft Matter*, 2012, **8**, 9079–9085.

7 Z. L. Chu and Y. J. Feng, *Chem. Commum.*, 2010, **46**, 9028–9030.

8 Y. G. Zhang, Y. J. Feng, Y. J. Wang and X. L. Li. *Langmuir,* 2013, **29**, 4187–4192.

9 Y. M. Zhang, J. Feng, Y. J. Wang, S. He, Z. R. Guo, Z. L. Chu and C. A. Dreiss. *Chem. Commun.*, 2013, **49**, 4902–4904.

10 K. Tsuchiya, Y. Orihara, Y. Kondo, N. Yoshino, T. Ohkubo, H. Sakai and M. Abe, *J. Am. Chem. Soc.*, 2004, **126**, 12282–12283.

11 C. C. Liu and J. C. Hao, *J. Phys. Chem. B.*, 2011, **115**, 980–989.

12 Y. X. Han, Y. J. Feng, H.Q. Sun, Z. Q. Li, Y. G. Han and H.Y. Wang, *J. Phys. Chem. B,* 2011, **115**, 6893–6902.

13 K. Singh, Z. Toole, A McLachlan and D. G. Marangoni, *Langmuir*, 2014, **30**, 3673–3680.

14 L. J. Jiang, K. Wang, F. K. Ke, D. H. Liang and J. B. Huang. *Soft Matter*, 2009, **5**, 599–606.

15 Y. M. Zhang, Y. X. Han, Z. L. Chu, S. He, J. C. Zhang and Y. J. Feng, J. Colloid Interface Sci.,2013, **394**, 319–328.

16 R. A. Salkar, P. A. Hassan, S. D. Samant, V. V. Kumar, F. Kern, S. J. Candau and C. Manohar, *Chem. Commun.*, 1996, 1223–1224.

17 R. T. Buwalda, M. C. A. Stuart and J. B. F. N. Engberts, *Langmuir*, 2000, **16**, 6780–6786.

18 Y. Y. Lin, Y. Qiao, Y. Yan and J. B. Huang, *Soft Matter*, 2009, **5**, 3047–3053.

19 S. K. Saha, M. Jha, M. Ali, A. Chakraborty, G. Bit and S. K. Das, *J. Phys. Chem. B*, 2008, **112**, 4642–4647.

20 S. R. Raghavan and E. W. Kaler, *Langmuir*, 2001, **17**, 300–306.

21 G. C. Kalur, B. D. Frounfelker, B. H. Cipriano, A. I. Norman and S. R. Raghavan, *Langmuir*, 2005, **21**, 10998–11004.

22 L. Sreejith, S. Parathakkat, S. M. Nair, S. Kumar, G. Varma, P. A. Hassan and Y. Talmon, *J. Phys. Chem. B,* 2011, **115**, 464–470.

23 S. C. Sharma, L. K. Shrestha, K. Tsuchiya, K. Sakai, H. Sakai and M. Abe, *J. Phys. Chem. B*, 2009, **113**, 3043–3050.

Soft Matter Accepted Manuscript

24 D. Varade, K. Ushiyama, L. K. Shrestha and K. Aramaki, *J. Colloid Interface Sci.,* 2007, **312**, 489–497.

25 S. C. Sharma, L. K. Shrestha, K. Sakai, H. Sakai and M. Abe, *Colloid Polym. Sci.*, 2010, **288**, 405–414.

26 R. G. Shrestha, K. Sakai, H. Sakai and M. Abe, *J. Phys. Chem. B*, 2011, **115**, 2937–2946.

27 M. Abe, K. Tobita, H. Sakai, K. Kamogawa, N. Momozawa, Y. Kondo and N. Yoshino, *Colloids Surf., A*, 2000, **167**, 47–60.

28 A. L. Fameau, A. Arnould, A. Saint-Jalmes, *Curr. Opin. Colloid In,* 2014, **19**, 471–479.

29 D. Danino, D. Weihs, R. Zana, G. Ora, G. Lindblom, M. Abe and Y. Talmon, *J. Colloid Interface Sci*., 2003, **259**, 382–390.

30 R. Kumar, G. C. Kalur, L. Ziserman, D. Danino and S. R. Raghavan, *Langmuir*, 2007, **23**, 12849–12856.

31 Z. Chu, Y. Feng, H. Sun, Z. Li, X. Song, Y. Han and H. Wang, *Soft Matter*, 2011, **7**, 4485–4489.

32 H. Chen, Z. B. Ye, L. J. Han, P. Y. Luo and L. Zhang, *Surface Science*, 2007, **601**, 2147–2151.

33 M. M. Fredric and S. K. Jason. *Angew. Chem. Int, Ed.*, 2000, **39**, 1906–1920.

34 R. J. Zana, *J. Coll. Inter. Sci.*, 2002, **246**, 175-181.

35 M. Rosen and F. J. Li, *J. Coll. Inter. Sci.*, 2001, **234**(2), 418- 424.

36 X. L. Wei, X. H. Wang, D. Z. Sun, J. F. Liu, J. Liu, Y. H Sha and Z. N. Wang, *Soft Matter*, 2012, **8**, 10115–10122.

37 Z. B. Wei, X. L. Wei, D. Z. Sun, J. Q. Liu and X. J. Tang, *J. Coll. Inter. Sci.*, 2011, **354**, 677–685.

38 X. M. Pei, J. X. Zhao, Y. Z. Ye, Y. You and X. L. Wei. *Soft Matter*, 2011, **7**, 2953–2960.

39 P. A. Hassan, B. S. Valaulikar, C. Manohar, F. Kern, L. Bourdieu and S. J. Candau, *Langmuir*, 1996, **12**, 4350–4357.

40 J. Narayanan, E. Mendes and C. Manohar, *Int. J. Mod. Phys .B*, 2002, **16**, 375–382.

41 E. Mendes, R. Oda, C. Manohar and J. Narayanan, *J. Phys.Chem. B*, 1998, **102**, 338–343.

42 K. Horbaschek, H. Hoffmann and C. Thunig, *J. Colloid Interface Sci*., 1998, **206**,

Soft Matter Accepted Manuscript

439–456.

43 L. J. Magid and J. C. Gee, Y. Talmon, *Langmuir*, 1990. **6**, 1609–1613.

44 T. S. Kim, T. Kida, Y. Nakatsuji, T. Hirao and I. Ikeda, *J. Am. Oil. Chem. Soc.*, 1996, **73**, 67–71.

45 N. Mohmeyer and H. W. Schmidt, *Chem. Eur. J.*, 2005, **11**, 863–872.

46 L.X. Jiang, Y. Yan and J.B. Huang, *Soft Matter*, 2011, **7**, 10417–10423.

47 D. Wang, J. C. Hao, *Colloid Polym Sci.*, 2013, **291**, 2935–2946.

48 G. Ronsin, A. J. Kirby, S. Rittenhouse, G Woodnutt and P. Camilleri, *J. Chem. Soc., Perkin Trans*, 2002, **2**, 1302–1306.

49 G. Montalvo, M. Valiente and E. Rodenas, *Langmuir*, 1996, **12**, 5202–5208.

50 M. Doi and S. F. Edwards, *The theory of polymer synamic*, Clarendon, Oxford, UK, 1986.

Soft Matter Accepted Manuscript

Thermo-responsive properties driven by hydrogen bonding in aqueous cationic gemini surfactant systems

Figure Captions

Scheme 1 Chemical structures of cationic gemini surfactants n-3(OH)-n(2Cl), n = 12, 14, and 16

Fig. 1 Zero-shear viscosity of the n-3(OH)–n(2Cl) solution as a function of temperature at different concentrations

Fig. 2 Appearance of aqueous 200 mmol·kg^{-1} 14-3(OH)-14(2Cl), (a) 25°C, (b) 27°C, and (c) 32°C

Fig. 3 Dynamic frequency spectra and fitting curves according to the Maxwell model for 200 mmol·kg^{-1}14–3(OH)–14(2Cl) solution at 23°C

Fig. 4 Cryo-TEM images of solutions at 25ºC, (a) 200 mmol·kg^{-1} 14-3(OH)–14(2Cl) and (b) 150 mmol·kg^{-1}16-3(OH)–16(2Cl). Arrows indicate some micelle end points

Fig. 5 Mechanism of micellar formation in the 14–3(OH)–14(2Cl) solution at low and high temperatures

Fig. 6 Macroscopic appearances of 150 mmol·kg^{-1} 16–3 (OH)–16(2Cl) solution at different temperatures, (a) 30°C, (b) 31°C, and (c) 35°C

Fig. 7 Electric conductivity of 16-3(OH)–16(2Cl) solutions as a function of temperature at different concentrations

Fig. 8 Dynamic rheological curves of the100 mmol·kg^{-1}16-3(OH)–16(2Cl) solution as a function of temperature, (a) heating process; (b) cooling process

Fig. 9 (a) Stress and (b) frequency sweep curves of a 150 mmol·kg^{-1} 16–3 (OH)–16(2Cl) solution at 30°C, 31°C, and 35°C

Soft Matter Accepted Manuscript

Fig. 10 DSC heating and cooling curves of aqueous solutions of 16–3(OH)–16(2Cl) at 100 mmol·kg^{-1}

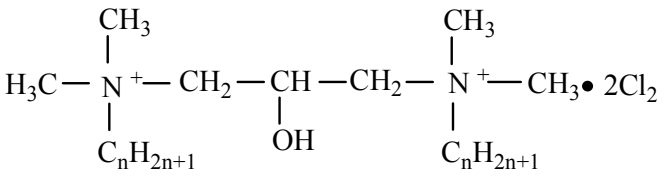

Scheme 1 Chemical structures of cationic gemini surfactants n-3(OH)-n(2Cl), n = 12, 14, and 16

Soft Matter Accepted Manuscript

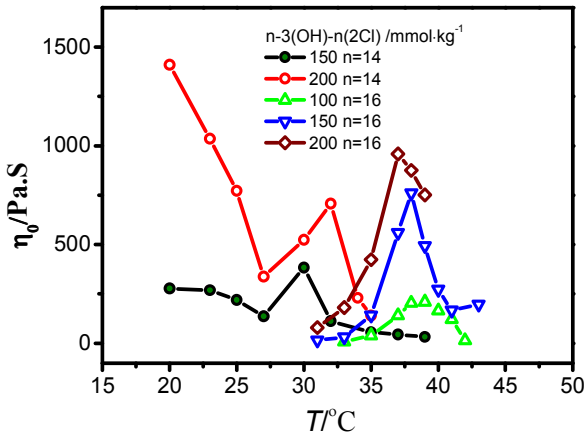

Fig. 1 Zero-shear viscosity of the n-3(OH)–n(2Cl) solution as a function of temperature at different concentrations

Soft Matter Accepted Manuscript

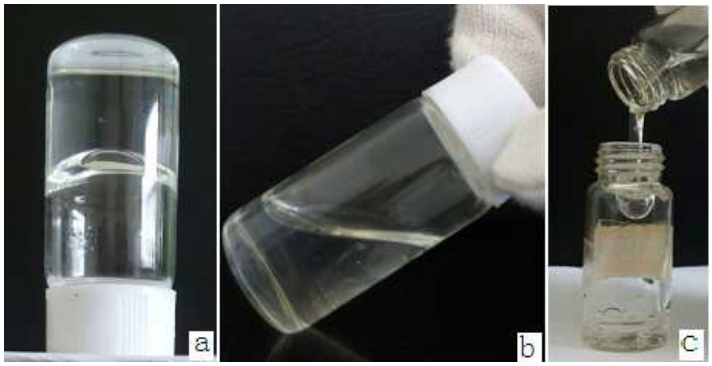

Fig. 2 Appearance of aqueous 200 mmol·kg^{-1} 14-3(OH)-14(2Cl), (a) 23°C, (b) 27°C, and (c) 32°C

Soft Matter Accepted Manuscript

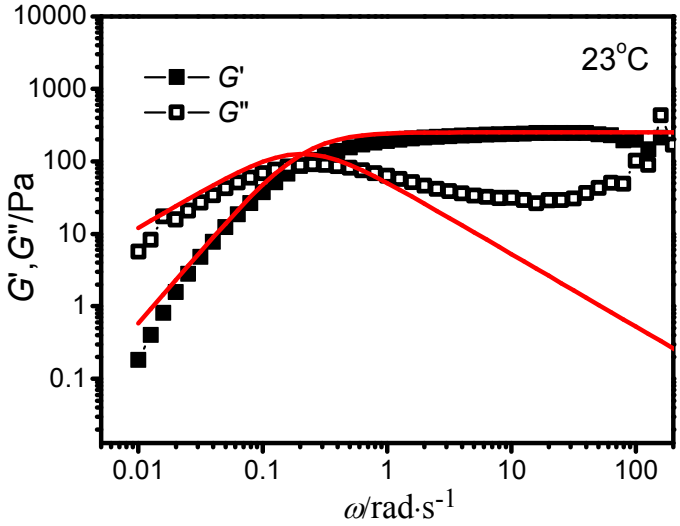

Fig. 3 Dynamic frequency spectra and fitting curves according to the Maxwell model for 200 mmol·kg^{-1}14–3(OH)–14(2Cl) solution at 23°C

Soft Matter Accepted Manuscript

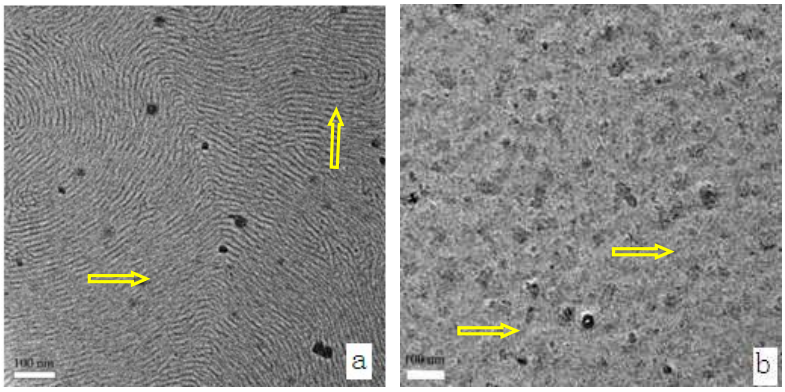

Fig. 4 Cryo-TEM images of solutions at 25ºC, (a) 200 mmol·kg^{-1} 14-3(OH)–14(2Cl) and (b) 150 mmol·kg^{-1}16-3(OH)–16(2Cl). Arrows indicate some micelle end points

Soft Matter Accepted Manuscript

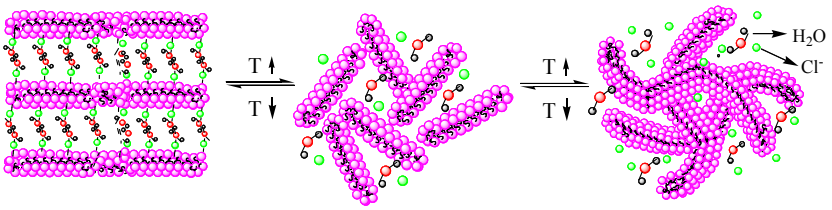

Fig. 5 Mechanism of micellar formation in the 14–3(OH)–14(2Cl) solution at low and high temperatures

Soft Matter Accepted Manuscript

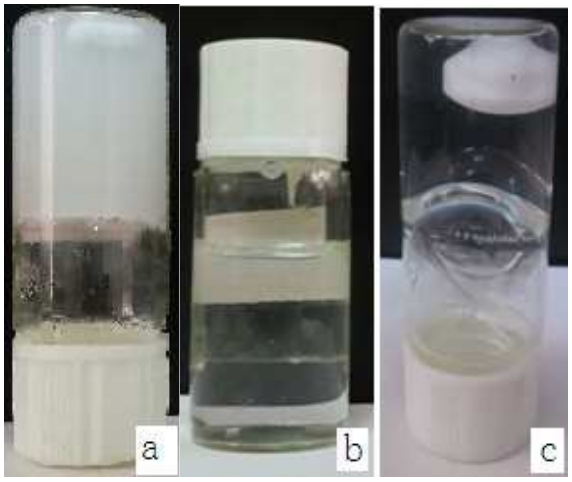

Fig. 6 Macroscopic appearances of 150 mmol·kg^{-1} 16–3 (OH)–16(2Cl) solution at different temperatures, (a) 30°C, (b) 31°C, and (c) 35°C

Soft Matter Accepted Manuscript

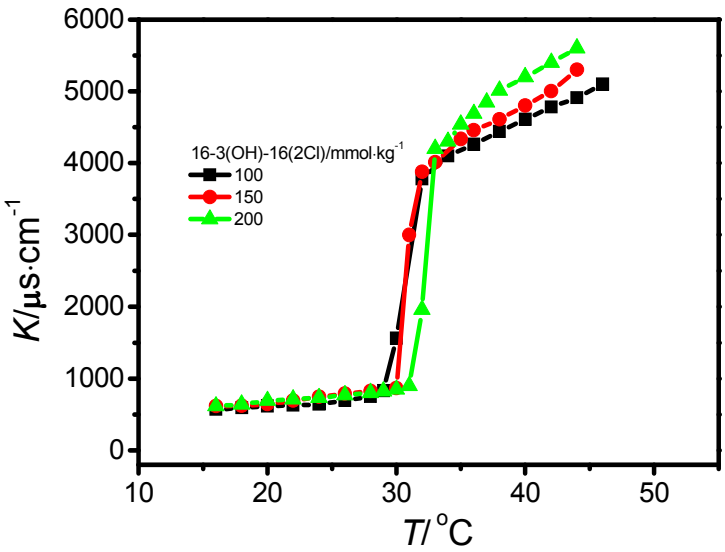

Fig. 7 Electric conductivity of 16-3(OH)–16(2Cl) solutions as a function of temperature at different concentrations

Soft Matter Accepted Manuscript

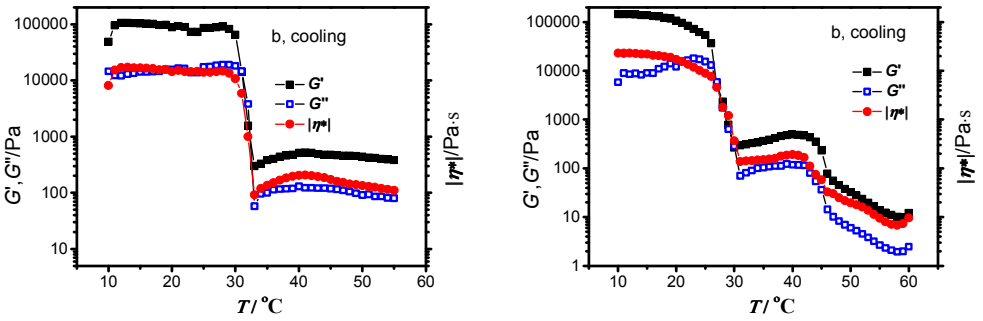

Fig. 8 Dynamic rheological curves of the100 mmol·kg^{-1}16-3(OH)–16(2Cl) solution as a function of temperature, (a) heating process; (b) cooling process

Soft Matter Accepted Manuscript

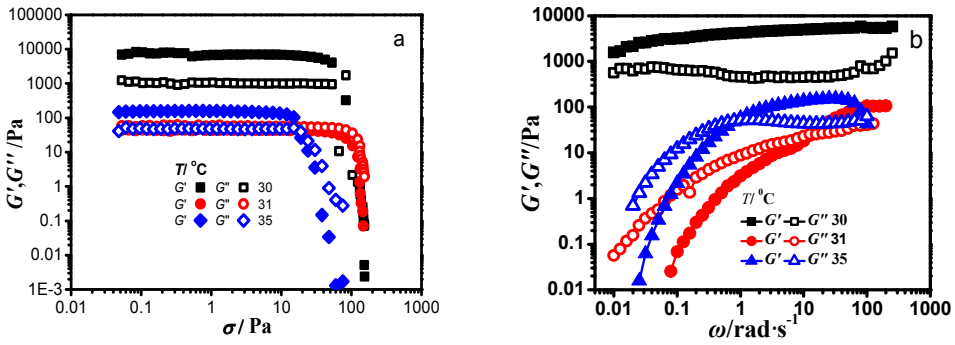

Fig. 9 (a) Stress and (b) frequency sweep curves of a 150 mmol·kg^{-1} 16–3 (OH)–16(2Cl) solution at 30°C, 31°C, and 35°C

Soft Matter Accepted Manuscript

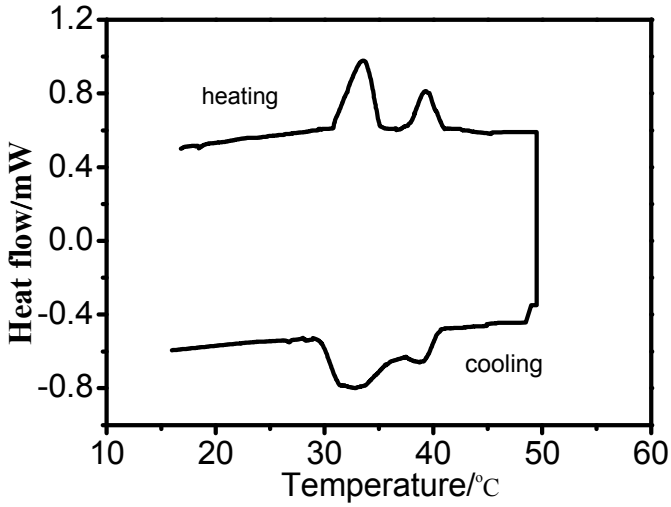

Fig. 10 DSC heating and cooling curves of aqueous solutions of 16–3(OH)–16(2Cl) at 100 mmol·kg^{-1}

Soft Matter Accepted Manuscript

Table 1. T_{gel} and Some rheological parameters of 16–3(OH)–16(2Cl)/NaCl mixed solution

Number	C_{NaCl} mmol·kg^{-1}	T_{gel} °C	η_0 /Pa·s		G_0/Pa		t_R/s	
			hydrogel	solution	hydrogel	solution	hydrogel	solution
1	20	36	52.89	3.923	22880	1.336	∞	1.585
2	40	37	13.42	1.917	15090	1.491	∞	2.893
3	60	38	8.392	1.264	525	1.407	∞	3.059
4	80	39	9.349	1.441	493	1.265	∞	4.435

Soft Matter Accepted Manuscript

Graphical abstract

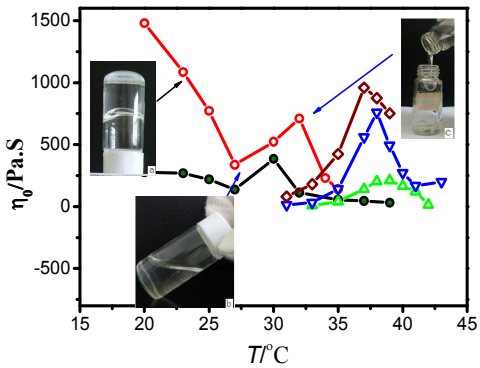

A series of thermo-response phenomena were discovered in the cationic surfactants (n-3(OH)-n(2Cl) and its aqueous solution with an inorganic salt

Soft Matter Accepted Manuscript